Joint Centre for Mesoscale Meteorology, Reading, UK

Attribution Concepts Applied To The Omega Equation

S. A. Clough
C. S. A. Davitt
A. J. Thorpe

Internal Report No. 47

June 1995

Met Office Joint Centre for Mesoscale Meteorology Department of Meteorology
University of Reading PO Box 243 Reading RG6 6BB United Kingdom
Tel: +44 (0)118 931 8425 Fax: +44 (0)118 931 8791
www.metoffice.com

Designed and produced by the Met Office © Crown copyright 2001 01/0240 The Met Office logo is a registered trademark.

ATTRIBUTION CONCEPTS APPLIED TO THE OMEGA EQUATION

by

S A Clough[1]*, C S A Davitt* and A. J Thorpe**
Joint Centre for Mesoscale Meteorology,
*UK Meteorological Office / **University of Reading, UK.

13 June 1995

ABSTRACT

Attributing synoptic development and structure to particular atmospheric features is an important practical problem. In this paper methods which have been proposed for the attribution of quasi-geostrophic potential vorticity (PV) are extended to the study of sources of vertical motion and the influence of the earth's surface and tropopause.

It is shown that in the presence of an exponential variation of density in the vertical both the PV and omega equations are governed by an identical form of Helmholtz's equation with a simple radially symmetric Green's function in layers of constant Brunt-Vaisälä frequency.

Analytical solutions are given and used to investigate the influence of boundary conditions and source (PV and div $\underline{Q}$) distributions, which distinguish the attribution of geopotential and vertical motion. In particular, solutions to the omega equation are markedly affected by dipole cancellation due to the surface boundary condition. The following results are shown:

- The compressible response to forcing suffers an exponential decay with range compared to the incompressible solution, with a deformation radius of order 2000 km in the mid-latitude troposphere. This behaviour characterises quasi-geostrophic PV inversion, and is most important in high latitudes.
- In the absence of boundaries, the incompressible solution correctly represents the response at levels above a source, but overestimates the response beneath the source in proportion to the density.
- Because of the surface dipole cancellation the incompressible solution to the omega equation is accurate for most purposes.
- The effects of lower level sources of vertical motion (below 700 hPa) are shown to be inhibited and highly localised.
- The tropopause causes only a small dipole cancellation in the omega equation, while the tropospheric response to stratospheric sources is strongly inhibited.

It is concluded from the above results that upper tropospheric and tropopause-level sources tend to dominate the large scale pattern of vertical motion. Green's function formulation of the problem also suggests source-based approaches to practical diagnostic study which can be related to the above properties.

---

[1]Corresponding author: Joint Centre for Mesoscale Meteorology, Harry Pitt Building, University of Reading, Whiteknights Road, PO Box 240, Reading, RG6 2FN, UK. (The Joint Centre for Mesoscale Meteorology is supported by the Meteorological Office and the Department of Meteorology, University of Reading.)

1. INTRODUCTION

Because of the very different technical disciplines encompassed by meteorology, communication can be a major obstacle to the practical introduction and application of new ideas. This is nowhere more evident than in forecasting large scale weather. The solution of partial differential equations is a central part of the conceptual problem of theory, while practicing forecasters are not usually mathematicians trained in fluid mechanics but physicists interpreting observations. A possible means of reducing this communication gap is the use and emphasis of principles which are part of the early training common to physical scientists.

One of these principles is the idea of "action at a distance", a property of systems governed by linear partial differential equations such as Poisson's equation. This concept is essential in electrostatics theory, where the total electric field at a point in a domain is the sum of the fields from individual point charges in the domain. This has its parallel in the study of weather systems in attempting to attribute the distribution of geopotential or vertical motion to specific sources. Conventional language identifies sources, for example, in terms of troughs, potential vorticity anomalies or thermal and vorticity advection whereas an important aim of theoretical work is to unify and simplify to a minimal appropriate description. Towards this end Bishop and Thorpe (1994) (hereafter referred to as BT) and Thorpe and Bishop (1995) have proposed an electrostatics analogy for potential vorticity (PV) in which the geopotential field at a point is viewed as the superposition of fields from individual point sources of PV; the mathematical methods of electrostatics then provide simple and lucid means of representing the effects of the earth's surface and tropopause.

The attribution of geopotential to quasi-geostrophic PV relies upon the resemblance of the governing equation to Poisson's equation. This approach can be extended to vertical motion because the omega equation has a similar form, the source of vertical velocity being given in terms of div $\underline{Q}$, the horizontal divergence of the $\underline{Q}$ vector (defined by Hoskins, Draghici and Davies (1978)). This extension is the main topic of the present work. The attribution of vertical motion in weather systems is an important practical problem in weather forecasting and numerical modelling, because it is important to know how particular upper or lower level features might contribute to the precipitation and evolution of a weather system. Further works will be concerned with the practical application of the approach, but here the essential principles are derived and some simple illustrative cases considered.

It should be noted that the operation of action at a distance is often implicitly ignored in meteorology. This occurs, for example, in studies of the omega equation, such as Hoskins, Draghici and Davies (1978) and following work, where div $\underline{Q}$ at one level (typically 700hPa) is often regarded as a surrogate for the vertical velocity at that level. While this may be reasonable first approximation in some cases, it must be subject to reservations since values of div $\underline{Q}$ are typically much larger at low levels and the tropopause than in mid-troposphere where there are smaller temperature gradients (Clough and Davitt (1994)).

The attribution approach provides a natural formalism for expressing these ideas, and potentially distinguishing the effects of rival forcing processes, eg. the presence of upper and lower level perturbations, diabatic heating and friction. Linear superposition of solutions is possible within the quasi-geostrophic system, and the Green's function methodology presents an effective means of working in terms of responses to local forcing and explicit representation of the effects of boundary conditions. As the solution to forcing from a point source it can be used formally to construct the geopotential or vertical velocity response to any internal or boundary source distribution of forcing.

In attempting to apply the electrostatics analogy of BT to both equations in a unified manner, it was found that for both PV inversion and the omega equation the extension of the analogy leads, apparently fortuitously, to an identical Helmholtz equation (rather than Poisson's equation), for the case of a compressible fluid layer of constant Brunt-Vaisälä frequency. Thus a common mathematical treatment can fruitfully be applied to both equations. The charge, source or forcing term in the former equation is provided by the potential vorticity, while for the latter it is proportional to div $\underline{Q}$. This is developed in Section 2.

In practice, of course, the spectral properties of source or forcing distributions for the geopotential and vertical velocity are very different, and these different patterns are essential to the character of synoptic development. Potential vorticity is approximately conserved for substantial periods, and positive anomalies especially can maintain their integrity because they can exert control over the flow field, so that they often have scales comparable to the Rossby radius of deformation. Patterns of forcing for the omega equation, on the other hand, are rapidly changing with time and can have appreciable structure on small scales, such as bands and dipoles (Keyser, Reeder and Reed (1988), Clough and Davitt (1994)).

While these differences of forcing do lead to quite different patterns of geopotential and vertical motion, some of the basic properties of the solutions arise from the different boundary conditions for the two equations. These are the subject of the remainder of the paper, in which we discuss the occurrence of solutions for idealised sources of increasing complexity to highlight their practical implications.

As a result we suggest that it is helpful to recognise the operation of these general principles cumulatively as a background against which to view the structure of individual weather systems. That is, the overall behaviour of any system is constrained by the properties of the fundamental solution, as modified by the boundary conditions, since these determine and limit the response to a given distribution of forcing. The constraints are the focus of the present work, while the detailed forcing patterns will be considered in a further work.

2. THE COMPRESSIBLE EQUATIONS AND THEIR SOLUTION

First the two basic equations, the omega equation and the equation for the quasi-geostrophic potential vorticity, are compared in order to demonstrate the similarity between their solutions. The compressible form of the quasi-geostrophic omega equation may be written as

$$N^2\nabla_h^2 w + f_0^2\frac{\partial}{\partial z}\left(\frac{1}{\rho_s}\frac{\partial}{\partial z}(\rho_s w)\right) = 2\nabla_h\cdot\underline{Q} \qquad (1)$$

where z is the height-like pressure coordinate of Hoskins and Bretherton (1972), w is the vertical velocity dz/dt, N is a reference Brunt-Vaisälä frequency dependent on height only, ρ_s is the reference density profile and f_0 is the Coriolis parameter. $\underline{Q}$ is the rate of change of the potential temperature gradient following the geostrophic flow, first defined by Hoskins, Draghici and Davies (1978), and ∇_h is the horizontal gradient operator on constant z surfaces.

It is shown in Appendix 1 that this equation and the compressible equation for the quasi-geostrophic potential vorticity Eq. (2) may both be written in a suitable form to parallel the electrostatics analogy of BT. However, it can be seen from Eqs. (A1.5) and (A1.7) that the vertical variation of density corresponds to a medium with continuously varying dielectric constant. In this section it is demonstrated that an analytical solution is still possible for both the omega equation and potential vorticity inversion in the important special case of an exponentially varying density profile with constant N.

For a potential vorticity perturbation $q-q_{ref}$ in a background field $q_{ref}=f$ the equation for the quasi-geostrophic potential vorticity takes the form

$$\nabla_h^2\psi' + \frac{f_0^2}{\rho_s}\frac{\partial}{\partial z}\left(\frac{\rho_s}{N^2}\frac{\partial\psi'}{\partial z}\right) = q-q_{ref} \qquad (2)$$

where $\psi'=\phi'/f_0$ is the perturbation geostrophic streamfunction and ϕ' is the geopotential. For an atmospheric layer with constant N^2 and an exponential density profile

$$\rho_s = \rho_0\exp\left(-\frac{z}{H_\rho}\right) \qquad (3)$$

with scale height H_ρ it is readily but surprisingly found that both Eq. (1) and Eq. (2) reduce to the form

$$L\chi = F \qquad (4)$$

where the operator L is defined as

$$L = \nabla_h^2 + \frac{f_0^2}{N^2}\left(\frac{\partial^2}{\partial z^2} + \frac{\partial \ln \rho_s}{\partial z}\frac{\partial}{\partial z}\right)$$
$$= \nabla_h^2 + \frac{f_0^2}{N^2}\left(\frac{\partial^2}{\partial z^2} - \frac{1}{H_\rho}\frac{\partial}{\partial z}\right) \qquad (5)$$

and the source is either

$$F = \frac{2\nabla.\mathbf{Q}}{N^2}$$

for the omega equation or else

$$F = q - q_{ref}$$

for PV inversion and χ is either the geostrophic stream function ψ' or the vertical velocity w respectively. For brevity the right hand side will be hereafter referred to as the forcing and the solution χ for both the omega and potential vorticity problems simply as the response.

Thus for the important special case of a layer of constant static stability and an exponential density profile the two problems are isomorphic. The above is rather a striking result, and implies that the solutions must correspond (ie. remain isomorphic) for problems composed of such piecewise layers. Because of this common form, the conclusions of this section apply equally to inversion of both the omega equation and the quasi-geostrophic PV. In practice, however, it will become evident below that the different boundary conditions for the two problems lead to quite different properties in most practical circumstances, though both can be understood and related by the methods used here.

For this continuously varying medium Eq. (4) in scaled coordinates with $z' = N/f_0\, z$ is close in form to Poisson's equation from electrostatics. For Poisson's equation, which BT apply to the incompressible case, the fundamental solution $g(\mathbf{r}|\mathbf{r}_s)$ (Stakgold (1968)) or Green's function for an unbounded domain (Morse and Feshbach (1953)) is simply the potential

$$g(\mathbf{r}|\mathbf{r}_s) = \chi = -\frac{1}{4\pi r} \qquad (8)$$

at $\mathbf{r}$ associated with a unit point charge at $\mathbf{r}_s$, where r is the separation. Morse and Feshbach (1953) show that the Green's function for a particular problem $G(\mathbf{r}|\mathbf{r}_s)$ can normally be expressed by appropriate linear combination of fundamental solutions to match the boundary conditions.

There are benefits in applying an electrostatics analogy if it ensures that interaction between charges is symmetrical, ie. $g(\mathbf{r}|\mathbf{r}_s)$ is symmetrical in the arguments $\mathbf{r}$

and $\mathbf{r}_s$ and thus is a function of distance only. In the case of the atmosphere this implies a framework in which the height (and thus density) of sources occurs explicitly in the forcing but not in the form of the response. This is possible only for equations governed by self-adjoint operators (see eg. Morse and Feshbach (1953)). In Eq. (5) only the terms involving z are not self-adjoint in form, but a self-adjoint equation can be achieved by means of the substitution

$$\tilde{\chi} = \chi \rho_0^{\frac{1}{2}} \exp\left(-\frac{z}{2H_\rho}\right) = \chi \rho_s^{\frac{1}{2}} \tag{9}$$

to obtain

$$\nabla_h^2 \tilde{\chi} + \frac{f_0^2}{N^2}\left(\frac{\partial^2 \tilde{\chi}}{\partial z^2} - \frac{\tilde{\chi}}{4H_\rho^2}\right) = F \rho_0^{\frac{1}{2}} \exp\left(-\frac{z}{2H_\rho}\right) \tag{10}$$

Rescaling Eq. (10) in the vertical by the change $z'=N/f_0\, z$ it may be seen that this is equivalent to the inhomogeneous Helmholtz equation

$$\nabla^2 \tilde{\chi} - \left(\frac{f_0}{2NH_\rho}\right)^2 \tilde{\chi} = F \rho_0^{\frac{1}{2}} \exp\left(-\frac{z' f_0}{2NH_\rho}\right) \tag{11}$$

which has the fundamental solution (Morse and Feshbach (1953), p.891)

$$g(\mathbf{r}|\mathbf{r}_s) = -\frac{1}{4\pi r}\exp\left(-\frac{f_0}{2NH_\rho} r\right) = -\frac{1}{4\pi r}\exp\left(-\frac{r}{D_\rho}\right) \tag{12}$$

Thus the Green's function for the modified problem of Eq. (11) in the unbounded domain takes a simple spherically symmetrical form, where $\mathbf{r}_s$ is the position vector of the source, $r=((x-x_s)^2+(y-y_s)^2+(N/f_0)^2(z-z_s)^2)^{1/2}$ in conventional vector notation and we define a deformation radius $D_\rho=2NH_\rho/f_0$ associated with the compressibility. Returning to the original variables the vertical velocity or streamfunction perturbation attributable to a point source of magnitude $Q=\lim_{b\to 0} q\, 4\pi b^3/3$ at height z_s, as used by BT, may be written as

$$\chi = \frac{Q\rho_0^{-\frac{1}{2}}}{4\pi r}\exp\left(\frac{z}{2H_\rho} - \frac{f_0}{2NH_\rho} r\right) \tag{13}$$

The simple radial form of the solution in this case is a special case arising from

the exponential form of the density profile, a good approximation in the atmosphere. It should be noted also, that although there are in practice many constraints upon the existence and use of exact Green's functions the method generalises to semi-geostrophic PV (Thorpe and Bishop (1995). However this is unlikely to be the case for more accurate dynamical approximations for general PV distributions. The main constraint is the existence of self-adjoint form, which provides an assurance of the existence and symmetry of Green's functions for a system; this is a strong constraint upon operators (the use of Green's functions in quantum mechanics, for example, is greatly facilitated by the fact that observables correspond to Hermitian operators, which are self-adjoint (Morse and Feshbach (1953))).

3. THE FUNDAMENTAL SOLUTION FOR POTENTIAL VORTICITY

The primary topic of this work is the omega equation, but it is helpful first to use the isomorphism between the two equations, which clarifies the major role of the boundary conditions and source distributions. The two problems are normally solved with mathematically different surface boundary conditions. Neumann type (ie. $\partial\chi/\partial z=0$) conditions are normally used for the potential vorticity problem, corresponding to a condition on the potential temperature, while Dirichlet conditions (ie. $\chi=0$), corresponding to a condition on the vertical velocity, are usual for the omega equation.[2]

We consider the PV problem first to show the influence of the compressibility upon the response, but also because the derivative condition does not localise the spatial response to forcing as strongly as the Dirichlet condition, and so the bounded solutions are better approximated by the fundamental solution (ie. the Green's function for the unbounded domain, see Morse and Feshbach (1953)).

The compressible solution (Eqs. (12), (13)) differs from the incompressible solution (Eq. (8)) in both vertical dependence and horizontal range of influence. In the horizontal, the compressibility has the effect of localising the response through the exponential decay with radius, which is characterised by the deformation radius for compressibility D_ρ defined in Eq. (12). This is illustrated in Fig. 1 as a function of Coriolis parameter and static stability, for a density scale height H_ρ of 10km (Note, however, that H_ρ is more typically of order 6 km in the stratosphere). For a typical Brunt-Vaisälä frequency in the troposphere of order $N\sim10^{-2}s^{-1}$, D_ρ is comparable to the main baroclinic wavelengths around 2000 km in the middle to high latitudes, reaching its smallest values in high latitudes where low static stability is likely to further accentuate the effects of increased rotation rate. For stratospheric values of order $N\sim2\text{-}3\times10^{-2}s^{-1}$ D_ρ is about 3000 km, and thus the effects of compressibility are significant also on the scale of the dominant Rossby waves.

---

[2] Here we note the mathematical difference in these conditions, but note that setting w=0 at the surface leads to a condition in potential temperature from the thermodynamic equation.

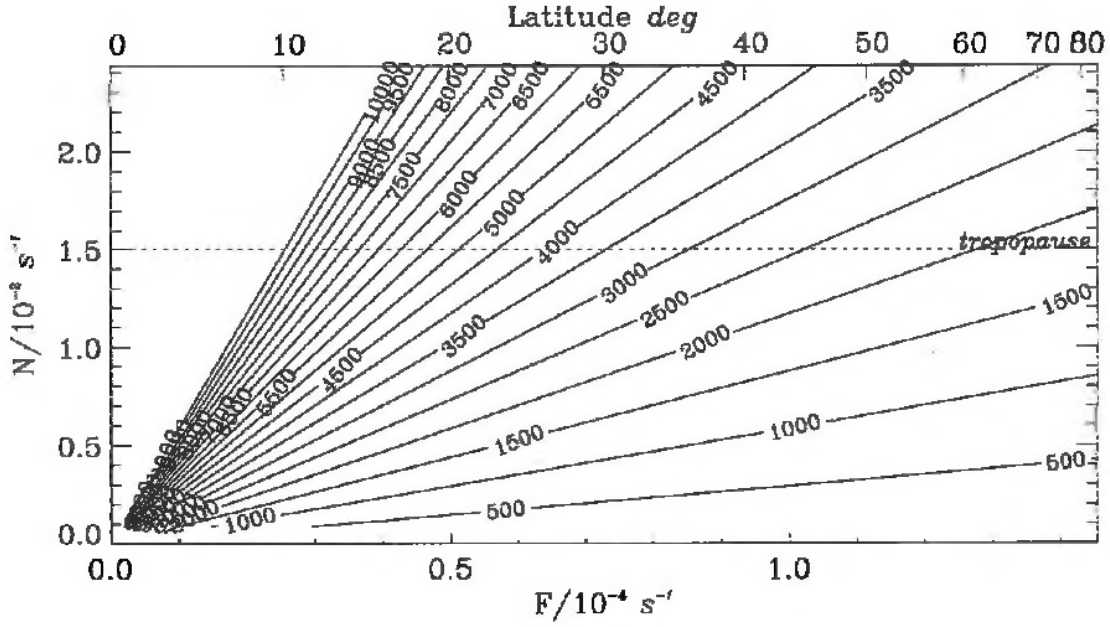

Figure 1 $D_p=2H_pN/f_0$, the deformation radius for compressibility, as a function of Coriolis parameter f_0 s^{-1} and Brunt-Väisälä frequency N s^{-1}, for H_ρ=10.2 km. Equivalent earth latitude is marked on the top axis, and the short dashed line indicates the approximate transition from tropospheric to stratospheric static stability values.

It is also evident from Eq. (12) that the response vertically above and below sources is distinguished by the varying density. Above the source point the two exponential terms exactly offset so that the response is identical to the incompressible response, whereas below the source the response is decreased by a factor $\exp(z-z_s/H_\rho)$, in proportion to the density.

These characteristics may be seen in Fig. 2, which shows the balanced vortex response attributable to ball-shaped PV anomalies q at three latitudes for both the incompressible and compressible cases. The corresponding analytical solution is given in Appendix 2. (It should be noted, however, that the two solutions are not quite comparable, because the density variation with height introduces a small bias term into the compressible problem for a finite ball, as discussed in the Appendix. This accounts for the different static stability variations in the source region.)

Fig. 2 shows the geopotential $\phi'=f_0\psi'$ and tangential wind fields calculated for compressible and incompressible ball anomalies $q=3\times10^{-4}f_{45}/f_0$ s^{-1} of radius 250 km at three different latitudes, in an unbounded atmosphere with $N^2=10^{-4}$ s^{-2} and density scale height H_ρ=10.2 km (these values are used for the troposphere in all following illustrations also). This specification of q corresponds at 45°N to that of BT, but maintains the same volume-integrated forcing as the latitude is changed. The plotting scales in this and subsequent Figs. have been chosen to give spherical symmetry in the scaled quasi-geostrophic coordinate at 45°N, as is evident in the incompressible

solution; for the compressible case spherical symmetry holds in the transformed variable $\tilde{\chi}$. For this unbounded case the height origin is arbitrary.

Figure 2 clearly shows the influence of the rotation rate in determining the quasi-geostrophic scaling and hence the aspect ratio and depth scale of the response, particularly in the velocity field. The vertical velocity from the unbounded omega equation is not illustrated, but has the same spatial pattern except that the amplitude, for a similarly defined source, varies as $1/f_0$ like the stream function. Thus the peak vertical velocity response to a fixed source is greatest in the lower latitudes; this is evident in Fig. 3 below.

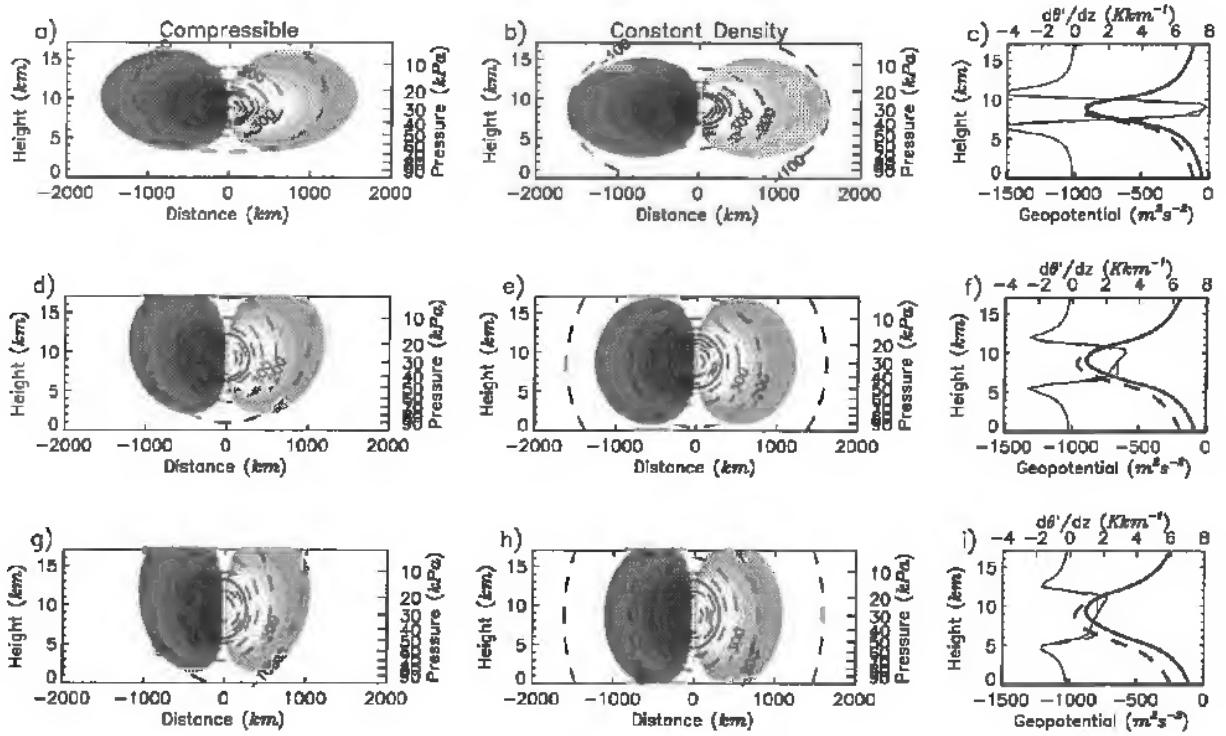

Figure 2 Solutions to the potential vorticity problem for ball sources q=3×10^{-4} f_{45}/f_0 of radius 250 km centred at 300hPa (z=8.6km) for an unbounded domain, row-wise at three latitudes: (a) geopotential (dashed contours at an interval 100m^{2}s^{-2}, solid contours at an interval 500m^{2}s^{-2}) and transverse wind component v (shaded between ±3ms^{-1} and ±6ms^{-1} at intervals of 1ms^{-1}, light shading into the plane, dark shading out of the plane) for the compressible case at 25°N (top row), (b) as (a) for the incompressible case, (c) corresponding vertical profile of geopotential (m^{2}s^{-2}, thick lines) and perturbation static stability $d\theta/dz$ Kkm^{-1} (thin lines) in a column through the source for the compressible case (solid) and the incompressible case (dashed); (d), (e), (f) as (a), (b), (c) respectively at 45°N; (g), (h), (i) as (a), (b), (c) respectively at 65°N.

The substantial localisation of the geopotential response due to compressibility is clearly evident, particularly in middle and high latitudes in Fig. 2(d) and 2(g), as well as an upward bias in the associated velocity distribution compared to the in-compressible case. It is interesting to note that this localisation is consistent with the observed prevalence of small-scale vortices in high latitudes compared to other locations. It is also consistent with the decline in eddy mean fluxes found by Williams (1988) on increasing the planetary rotation rate in a GCM. This decline was found to

occur progressively from high latitudes as the rotation rate was increased. This behaviour is consistent with our results, though no horizontal fields or other information are available on which to base a fuller comparison.

It is also evident in Fig. 2 that the differences in velocity between incompressible and compressible cases are less pronounced and more localised than in the geopotential response. This is to be expected for differentiated quantities, since the process of integrating the Poisson or Helmholtz problem smooths the effects of the localised disturbance out through large volumes to produce a response which differs most at long range because of the different intervening medium; differentiation inverts this delocalisation. Thus for most of the important derived quantities other than the geopotential itself the incompressible solution is an adequate approximation for many purposes.

4. THE EFFECTS OF BOUNDARIES AND TRANSITIONS

a) *The surface boundary condition in the omega equation*

The response to forcing is substantially modified by the presence of boundaries, in ways which can be given explicit representation using Green's functions. For geometrically simple boundaries such as plane surfaces the method of images can be simply used for many problems (Morse and Feshbach (1953)).

The approximate boundary condition normally used in solving the omega equation without orography is $w=0$ at $z=0$. In terms of the electrostatic analogy this corresponds to an assumption that the surface behaves as a conducting sheet. Unlike the case of PV inversion this condition does not depend upon secondary physical assumptions and there is no corresponding ambiguity in the interpretation of the omega equation, though further terms such as Ekman pumping or orographic forcing might be added. In using the method of images it should be noted that the method is purely a mathematical device for visualising the physical problem; however, it is also rigorous and economical in providing useful insights into the behaviour of solutions.

For a point source $2\nabla_h.Q/N^2$ of integrated magnitude S at a height z'_s, in quasi-geostrophic coordinates, the surface boundary condition is met by the addition of a negative image $-S$ at a height $z_i=-z_s$ so that the sum vanishes at the surface. Thus the Green's function for the incompressible problem becomes a vertically aligned dipole of strength $2Sz'_s$ and base length $2z'_s$ centred at z=0. Applying the properties of dipoles from electrostatics theory (Lorrain et al., (1988)), two important consequences follow.

Firstly, the dipolar cancellation due to the lower boundary introduces into the omega equation response a $1/r^2$ dependence, which localises the response towards small length scales and hence reduces the impact of compressibility upon the observed behaviour. For this reason there is no need to develop the analytical properties of the Helmholtz solution further for this problem, and we simply use illustrations to pursue our arguments.

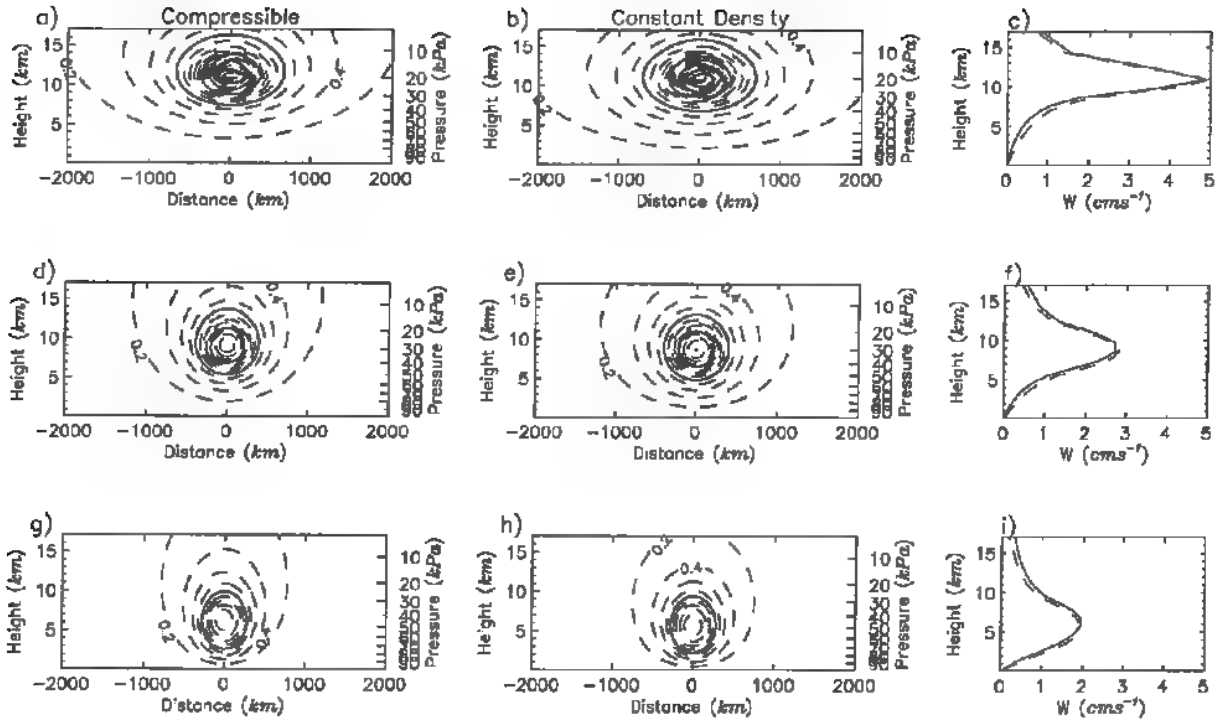

Figure 3 Vertical velocity distributions attributable to tropopause level sources $2\nabla_h.\underline{Q}/N^2 \ -10^{-14}f_{45}/f$ $m^{-1}s^{-3}$ as a function of latitude: (a) compressible case at 25°N (contours at intervals of 0.2 cms ^{1}(dashed), 1 cms^{-1} (full)), (b) as (a) for the incompressible case, (c) vertical profile through the source centre at 200hPa (11km) at 25°N, full line compressible, dashed line incompressible; (d), (e), (f) as (a), (b), (c) respectively for a source at 300hPa (8.6km) at 45°N;(g), (h), (i) as (a), (b), (c) respectively for a source at 500hPa (5.4km) at 65°N.

The similarity of the incompressible and compressible solutions is clearly evident in Fig. 3, which shows the vertical velocity attributable to a 250 km ball source $2\nabla_h.\underline{Q}/N^2$ of magnitude $2\nabla_h.\underline{Q}/N^2 - -10^{-14}f_{45}/f_0$ $m^{-1}s^{-3}$ placed at a level corresponding to the tropopause at three latitudes (with the same static stability for simplicity). The large difference between the long-range fundamental solutions, which was evident in Fig. 2, is lost by this dipolar cancellation. Even in this worst case of a troposphere-deep dipole the incompressible solution is adequate for practical purposes, particularly since the tropopause height is lowest in the high latitudes where compressibility effects are greatest.

The second implication of the dipole analogy is that the magnitude of the far-field ascent attributable to an isolated source is reduced in proportion to the height of the source z'_s because the baseline of the dipole is given by twice the source height. Thus the influence of isolated sources of vertical motion close to the surface is weaker and confined to much shorter ranges than upper tropospheric sources of vertical motion. This latter effect is clearly evident in Fig. 4, which shows the response at 45°N to identical sources at various levels (Note that the smaller sources are of increased magnitude to maintain the same integrated forcing as the 250 km sources.). Even at 700hPa (Fig. 4(d)-(f)) the far-field response is significantly reduced compared to that for forcing at 500hPa (Fig. 4(a)-(c).

This dipolar behaviour quantitatively amplifies the remark of Eliassen (1984) that the lower boundary condition causes the vertical velocity to reflect the local forcing, and appears to be an important geometrical influence on length scales in synoptic development. It is inherently a result of the operation of action at a distance, and thus arises more naturally in the Green's function approach than in the usual normal mode or wave-based conceptual model. Since development within systems is usually source-based and localised rather than part of a continuous wave-train this property is relevant to practical diagnosis and attribution of development.

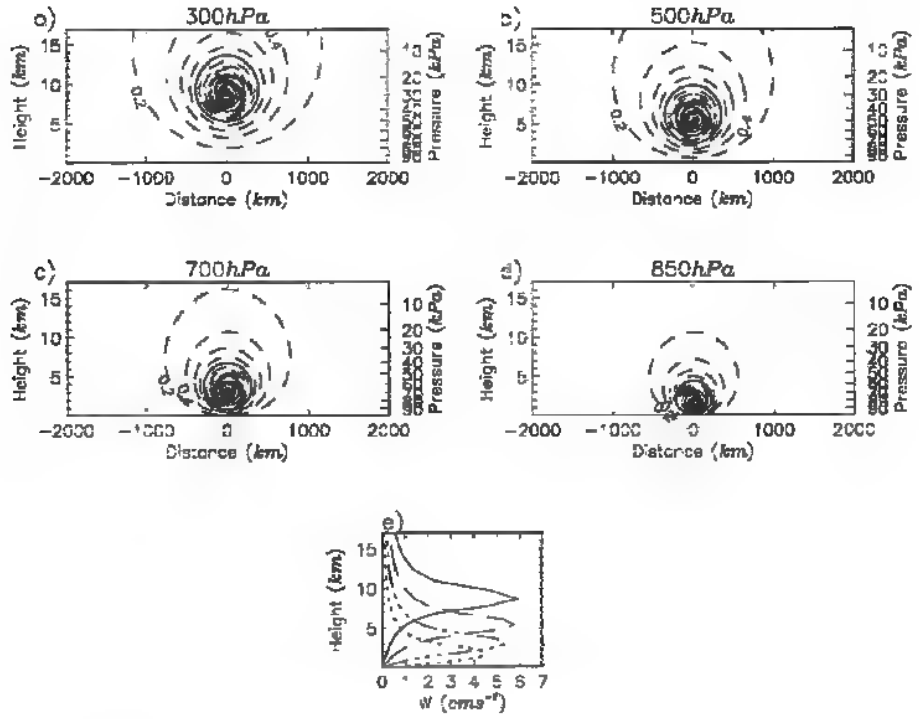

Figure 4 Vertical velocity distributions attributable at 45°N in a compressible atmosphere with surface boundary to 125 km ball sources $2\nabla_h.\Omega/N^2=-8\times10^{-14}$ $m^{-1}s^{-1}$ at (a) 300 hPa (8.6 km), (b) 500hPa (5.4 km), (c) 700 hPa (3 km), (d) 850 hPa (1.5 km). Contours are at intervals of 0.2 cm^{-1} (dashed), 1cms^{-1} (full), (e) profiles of vertical velocity through the source centre for cases (a)-(d).

b) *The surface condition in the potential vorticity equation*

The usual condition for inversion of a PV anomaly is that there is no temperature perturbation at the earth's surface associated with the vortex, ie. $\partial\psi/\partial z=0$. For a source S at height z_s this condition is satisfied by the addition of an image S at $-z_s$. Fig. 5 shows solutions to this problem for tropopause level sources at three latitudes. These may be compared with Fig. 2 (noting that the form of the geopotential response is independent of source height in Fig. 2) to show the influence of the boundary condition, which is obviously strongly localised to the boundary region beneath the source. As in the omega equation these effects are most important in mid-high latitudes because of the quasi-geostrophic scaling. Unlike the solution of the omega equation there is no dipolar cancellation so that there is a greater far field and compressibility remains quantitatively significant for PV inversion. Also, however, the localisation due to com-

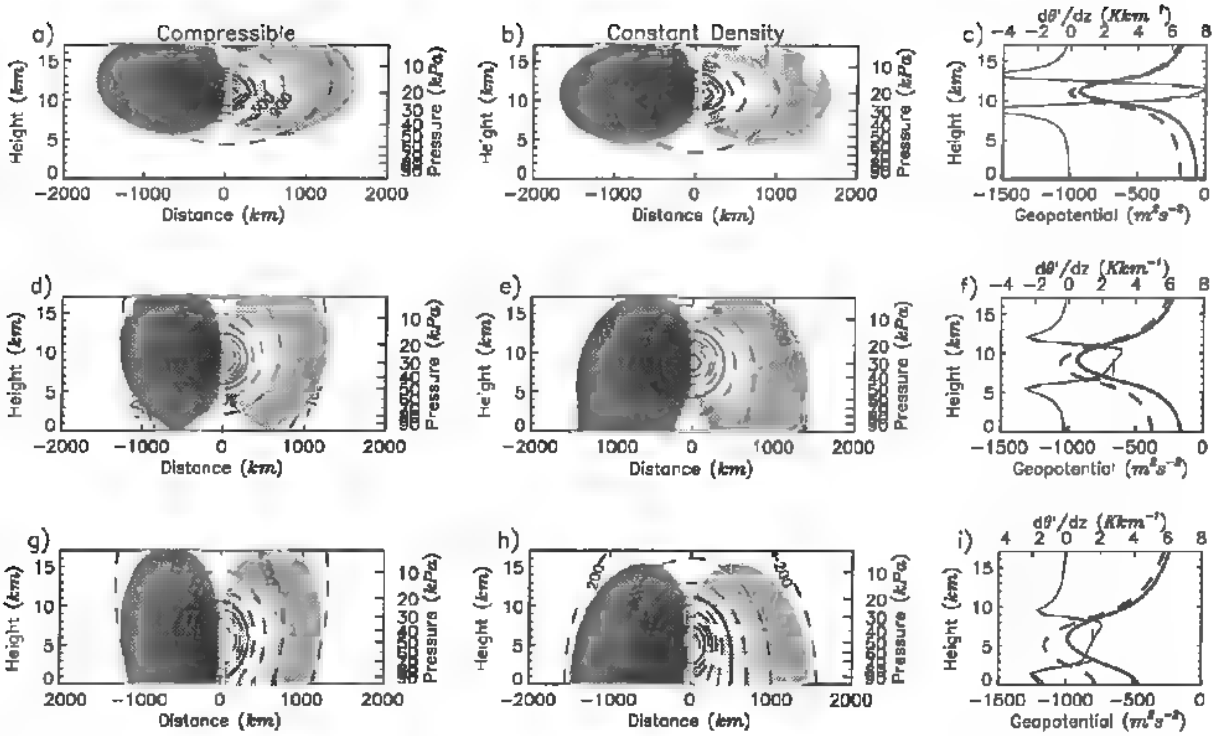

Figure 5 As Figure 2, but for tropopause level sources in a troposphere with inclusion of the surface boundary. Sources are at 200hPa (11km) at 25°N in (a), (b), (c); 300hPa (8.6km) at 45°N in (d), (e), (f); 500hPa (5.4 km) at 65°N in (g), (h), (i).

pressibility has a further effect; by reducing the far field it also reduces the effects of the subterranean image, so that the effects of the surface boundary condition are seen to be rather smaller in Figs. 5(a),(d) and (g) than in 5(b), (e) and (h). Thus the domain of influence of the lower boundary condition in PV inversion seems likely to be rather smaller than BT anticipated from the incompressible case, and this unbounded solution a correspondingly better approximation.

c) The influence of the tropopause

BT discuss in some detail the effect of the tropopause in the PV problem. For the compressible case simple solutions such as that exemplified by the method of images do not exist because of the continuously varying dielectric constant. While analytical solutions are probably attainable by asymptotic expansion this is not pursued here any further, as the incompressible case proves sufficient for our purpose.

The solution for the incompressible omega equation is similar to that of BT, except that the matching conditions of continuity of w and $\partial w/\partial z$ across the tropopause imply a negative contribution from a stratospheric image, and the corresponding solution is:

$$w_t = -\frac{Q}{4\pi}\left(\frac{1}{(x^2+y^2+z^2N_t^2/f_0^2)^{1/2}} - \frac{n}{(x^2+y^2+(z-2a)^2N_t^2/f_0^2)^{1/2}}\right)$$
$$w_s = -\frac{Q(1-n)}{4\pi}\left(\frac{1}{(x^2+y^2+(z-la)^2N_s^2/f_0^2)^{1/2}}\right) \qquad (14)$$

for a point source Q located at a distance a beneath the tropopause, where $n=l/m$, $l=(1-N_t/N_s)$ and $m=(1+N_t/N_s)$.

Fig. 6(a) shows such solutions for a source at 500hPa for a stratospheric value of $N_s^2=4\times10^{-4}s^{-2}$, for which the additional image has strength given by $n=-1/3$. However, it is readily seen by comparing Fig. 6(c) with Fig. 4(b) that the reduction of the far field due to the surface boundary condition already reduces the far field to such an extent that the tropopause condition for omega will have little further effect, except in the stratosphere.

It is also to be expected that the influence of stratospheric sources upon the

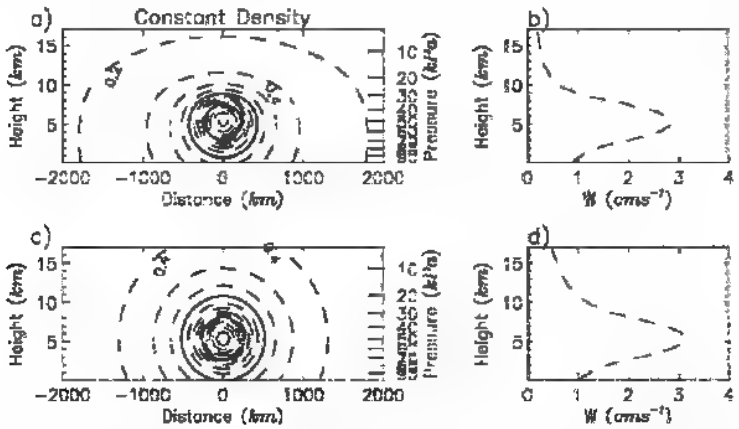

Figure 6 Vertical velocity distributions attributable to sources $2v_h.\Omega/N^2=-10^{14}$ $m^{-1}s^{-3}$ at 500hPa at 45°N for an incompressible atmosphere with $N_t^2=10^{-4}$ s^{-2} in the absence of a surface boundary condition. (a), for a stratospheric value $N_s^2=4\times10^{-4}s^{-2}$ above 300hPa. (contours at intervals of 0.2 cms^{-1} (dashed), 1 cms^{-1} (full)).(b) indicates the vertical velocity profile through the source centre corresponding to (a). (c), (d) as (a), (b)but in the absence of any stratosphere.

troposphere must diminish steadily with height above the tropopause. This arises not only from the sharp $1/r$ decay of the stratospheric Green's function but also from the density contribution to Eq. (13), particularly given the shallower density scale height in the stratosphere.

5. SOLUTIONS FOR SIMPLE SOURCE DISTRIBUTIONS

a) Multipole characteristics of forcing

Most practical circumstances are not adequately described by the simple single sources discussed above. Indeed, since the forcing is expressible in the form of a

divergence it is necessary that more than one source be present at some length scale. Multipole expansion is a helpful way of viewing complex distributions of charge in electrostatics (Lorrain et al., (1988)). Strictly, multipole expansions are most accurate at length scales considerably larger than those of the source distribution, but they are nonetheless instructive in this case. In practice, horizontal distributions of div $\underline{Q}$ tend to be dominated by dipolar or banded patterns, often on quite short length scales (Clough and Davitt (1994)). Such structure is less clearly evident in PV distributions, though a wind speed maximum might well be expected to be associated with a PV dipole since a jet maximum in a straight flow must be associated with low vorticity (and usually low potential vorticity) on its warm side as well as a positive PV anomaly on the cold side. However, the importance of positive anomalies is usually emphasised because they are usually dominant in development regions, and are more closely associated with the location of surface cyclone development.

Since the $\tilde{\chi}$ problem is isotropic in the scaled coordinate, the influence of a dipole pair of opposite sources $\pm Q$ separated by a distance $2s$ in the horizontal plane will possess a pattern similar to that associated with the lower boundary condition, but with horizontal axis. Clearly, as was found above, decreasing the separation of sources leads to a decrease in the amplitude and range of the resulting vertical motion, and the pattern of w tends to resemble that of -div $\underline{Q}$, as it would for a sinusoidal source distribution.

Fig. 7(a) shows the vertical motion fields associated with a dipole pair in the absence of boundaries. Comparing with Figs. 3 and 4 the reduction of the far field by cancellation can immediately be seen. This arises because the dominant length scale is the horizontal length scale provided by the dipole separation, 500 km. Since this is only half of the dipole length associated with the scaled source height the response to this dipolar forcing is more localised than implied by the source height alone.

However, as the dipole approaches the surface then a substantial further cancellation arises from the field associated with the oppositely aligned subterranean dipole image. Such a source tends to behave instead as a quadrupole centred at the surface; the dashed lines in Fig. 6 indicate the locus of positions corresponding to exact quadrupole behaviour for a symmetric dipolar div $\underline{Q}$ source. Since the far field response to a quadrupole decreases as $1/r^3$ (Lorrain et al., (1988)) the actual vertical motion field attributable to it will be rather small and thus further localised by the presence of the boundary. This behaviour is clearly evident in Fig. 6(b) and 6(c), where the images associated with the lower boundary condition are included for sources at 500hPa in (c) and (d), and 750hPa in (e) and (f). In cases (e) and (f) a highly localised response is found where the sources at 750hPa are located on the quadrupole locations.

This case is of particular interest because it commonly arises in the low level forcing of vertical motion near a developing cyclonic centre. In that region it is usually

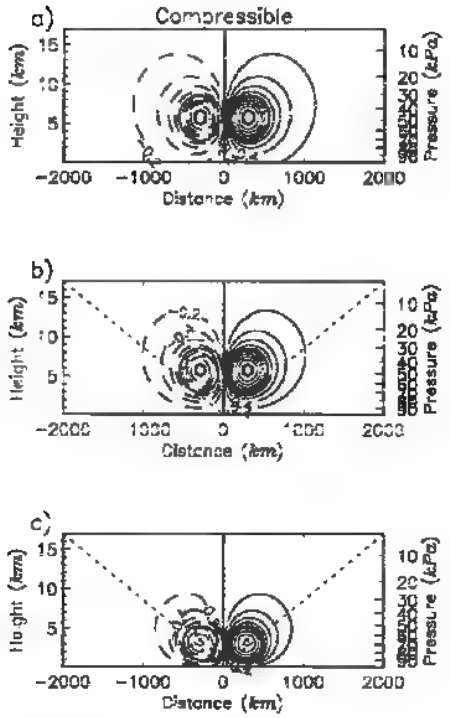

Figure 7 Vertical motion attributable to dipole source distributions $\pm 2\nabla_h \cdot Q/N^2$ 10^{-14}m^{-1}s^{-3} separated by 500km in the horizontal in a compressible atmosphere at 45°N. (a) shows sources placed at 500hPa (5.4km) in an unbounded atmosphere. (b) is as (a), but with the inclusion of a lower boundary at z=0. The lines $z'=\pm x$ are denoted by short dashes. (c) is as (b), but with sources at 750hPa (2.5km).

found that the horizontal pattern of div $\underline{Q}$ is approximately dipolar because of the changing advection in the cold front and warm front regions (eg., Clough and Davitt (1994)). The above considerations suggest that the vertical motion attributable to this configuration will be particularly localised and probably shallow.

b) Superposition of upper and lower forcing

Our earlier examples have shown that the vertical motion pattern in the mid-troposphere is substantially influenced by sources at other levels. In Fig. 8 we illustrate the vertical motion pattern resulting from a combination of upper and lower level ball sources. It is clearly evident here that the resulting vertical motion near the steering level, typically at 600-700 hPa, will in practice be rather sensitively determined by the detailed interplay between the two sources. A small change in the intensity or level of either source can make a marked difference in the vertical velocity; clearly as a system evolves these sources and their superposition change. Diagnosing these contributions separately during the development of weather systems is thus likely to be a valuable aid to the forecaster in interpreting the evolution of a model forecast.

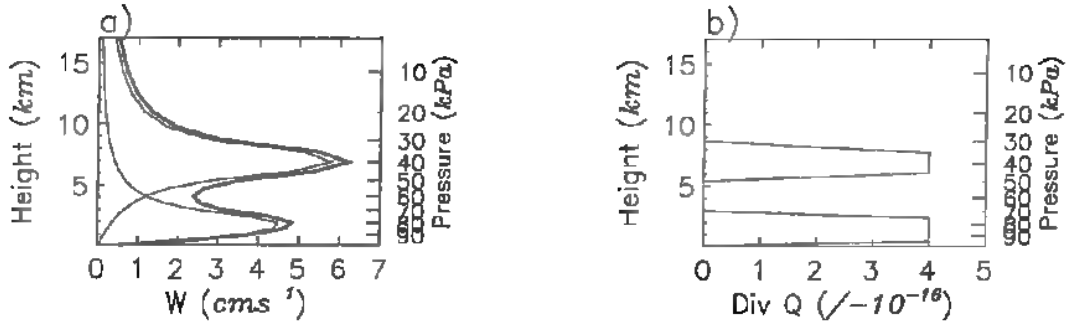

Figure 8 (a) Profiles of vertical velocity (cm s^{-1}) through the source points attributable to 125 km ball sources div $\underline{Q}$ at 400 hPa and 850 hPa individually (thin lines) and superposed (heavy line); (b) Profile of div $\underline{Q}$ ($m^{-1}s^{-1}$).

c) Vertical motion attributable to a PV anomaly

From the point of view of establishing the simplest building blocks for atmospheric dynamics, the case of a single point PV anomaly embedded in a uniform sheared (zonal) basic flow is now considered. The addition of the basic flow $\bar{u}(z)$, in thermal wind balance, to that attributable to a PV anomaly generates a div $\underline{Q}$ forcing pattern. In fact the forcing term is

$$F = \frac{f_0}{N^2} \frac{d\bar{u}}{dz} \frac{\partial \zeta}{\partial x}$$

so that the omega equation forcing term is proportional to the zonal gradient of the vorticity due to the PV anomaly. This forcing term is an asymmetrical sextupole, in which the dipole contribution is dominant. The omega equation and potential vorticity approaches can be linked more generally along the lines suggested by the appendix to Hoskins et al (1985), where the omega equation forcing is rewritten in terms of differential advection of potential vorticity, boundary temperature advection and isentropic upgliding.

Thus the simplest case of a single PV anomaly embedded in a uniformly sheared flow creates an essentially dipolar div $\underline{Q}$ forcing and an approximately dipolar vertical motion pattern.

4. CONCLUSIONS

The mathematical form of the quasi-geostrophic omega equation allows a simple electrostatics analogy to be made in which the vertical variations of density and static stability act as a dielectric "constant". This realisation allows several properties of the omega equation to be determined without recourse to particular solutions:

- Static compressibility causes a localisation of the omega pattern, determined by a compressible Rossby radius of deformation parameter, D_ρ, typically of order 2000 km in the mid-latitude troposphere and 3000 km in the stratosphere.

- The rigid surface condition, w=0, also produces a localisation with a "far-field" radial dependence of $1/r^2$ for a monopole forcing rather than the $1/r$ applicable to an infinite domain. This effect is important for omega, to the extent that the localisation due to compressibility may be neglected for most purposes.

- As div $\underline{\mathbf{Q}}$ forcing is typically dipolar this localisation involves a $1/r^2$ dependence for an infinite domain and $1/r^3$ if the rigid surface condition is included.

- For a tropospheric forcing the tropopause acts to reduce the omega response in the stratosphere.

- For a stratospheric forcing the increased static stability and compressibity effects together imply that, in practice, there will only be a small response in the troposphere.

It was also found that in the special case of an atmospheric layer with constant static stability and exponential density profile the governing equation for potential vorticity has exactly the same form as that for vertical motion. Thus the localisation associated with the compressible Rossby radius of deformation, D_ρ, also applies to the geopotential derived from quasi-geostrophic inversion of potential vorticity. Because Neumann derivative boundary conditions are normally used for this problem, no dipolar cancellation exists in the "far-field", and so in this case the localisation due to compressibility remains significant at synoptic scales, particularly at high latitudes. Because of this localisation the effects of the surface boundary condition for the inversion of PV appear to be less severe in practice than anticipated by Bishop and Thorpe (1994) for the incompressible case.

These results suggest that at the steering level, typically near 700hPa, the larger scale aspects of vertical motion must be dictated by upper-level div $\underline{\mathbf{Q}}$ sources. Equally, the smaller-scale detail in the vertical motion pattern tends to be dominated by lower level sources. This suggestion is based essentially upon geometrical constraints, and clearly the spatial characteristics of the forcing must also be considered in detail. This will be done in a following work, but our purpose here has been to separate these factors in order to carry out attribution in an appropriate way.

The emphasis of this study has been upon a 3-dimensional geometric view of diagnostic equations applied to weather systems, rather than the conventional approach to weather system development, which is usually focussed upon the source terms themselves and their origins in the local flow. While the source terms are clearly over-riding the response must be subject to the constraints discussed here, thus we suggest the importance of an intuitive understanding of the geometrical constraints imposed by the underlying equations and boundary conditions. Both of these are important and can be readily visualised and mathematically described using the methods of electrostatics or potential theory with little actual computation. The fronto-genetic mechanisms operating in individual weather systems may be more clearly viewed in this context, where weather system development can be associated with the redistribution of sources such that their cancellation or superposition is modified.

While much of the present work has been exploring some of the fundamental properties of the governing quasi-geostrophic equations, the central aim of the work is to provide diagnostic tools for understanding weather system development. Because the emphasis in diagnostic study is upon the spatial distribution of forcing associated with local sources the Green's function viewpoint seems to have some advantages for this purpose over the delocalised wave-like solutions used in most theoretical work on baroclinic development (notable exceptions being Charney (1963), Hogg and Stommel (1985a,b)). It also has the particular benefit that it can be used to generate formal solutions for a given forcing distribution to design practical tools for attribution, such as diagnostic measures of upper-level and lower-level forcing; a first demonstration of the approach was given by Clough and Davitt (1994) and further work is in progress.

It should be noted that our results also are only valid within the scope of quasi-geostrophic theory, and in the absence of orographic or other inhomogeneous boundary forcing terms, though Morse and Feshbach (1953) demonstrate that the latter can be dealt with by an extension of the methods used here. More accurate approaches are possible, for example use of the omega equation suggested by Eliassen (1984) for situations of increased baroclinicity, though despite their common use the quantitative validity of quasi-geostrophic predictions has not been widely tested. Since the inversion of the diagnostic relationships like the omega equation is straightforward with current computing resources (Clough and Davitt (1994)), this provides an effective means of testing the above principles in the context of a primitive equation model.

APPENDIX 1

The electrostatics analogy for compressible quasi-geostrophic equations

In order to generate for the omega equation an electrostatics analogy it is necessary to define a suitable vector field $\underline{D}$ comparable to the displacement vector such that Eq. (1) takes the form

$$\nabla.\underline{D} = \frac{2\nabla.\underline{Q}}{N_0^2} \qquad \text{(A1.1)}$$

where

$$\underline{D} = \left(\frac{\partial}{\partial x}\left(\frac{N^2}{N_0^2}w\right),\ \frac{\partial}{\partial y}\left(\frac{N^2}{N_0^2}w\right),\ \frac{f_0^2}{N_0^2}\frac{1}{\rho_s}\frac{\partial}{\partial z}(\rho_s w) \right) \qquad \text{(A1.2)}$$

where N_0 is a constant reference Brunt-Vaisälä frequency, noting that both N and N_0 are independent of x and y. Further, since the reference density profile ρ_s is also independent of x and y,

$$\underline{D} = \frac{\rho_0}{\rho_s}\left(\frac{N^2}{N_0^2}\frac{\partial}{\partial x}\left(\frac{\rho_s}{\rho_0}w\right),\ \frac{N^2}{N_0^2}\frac{\partial}{\partial y}\left(\frac{\rho_s}{\rho_0}w\right),\ \frac{f_0^2}{N_0^2}\frac{\partial}{\partial z}\left(\frac{\rho_s}{\rho_0}w\right) \right) \qquad \text{(A1.3)}$$

where ρ_0 is a constant reference density, ie.

$$\underline{D} = \underline{\underline{\epsilon}}\ \nabla\left(\frac{\rho_s}{\rho_0}w\right) \qquad \text{(A1.4)}$$

where $\underline{\underline{\epsilon}}$ is a diagonal permittivity tensor which is non-dimensional and has non-zero elements

$$\epsilon_{11} = \epsilon_{22} = \frac{\rho_0 N^2}{\rho_s N_0^2}$$
$$\epsilon_{33} = \frac{\rho_0 f_0^2}{\rho_s N_0^2} \qquad \text{(A1.5)}$$

In a similar way the potential vorticity equation, Eq. (2), may be written in the form

$$\nabla.\underline{D} = \frac{\rho_s}{\rho_0}(q - q_{ref}) \qquad \text{(A1.6)}$$

where

$$\underline{D} = \left(\frac{\rho_s}{\rho_0} \frac{\partial \psi'}{\partial x}, \frac{\rho_s}{\rho_0} \frac{\partial \psi'}{\partial y}, \frac{\rho_s f_0^2}{\rho_0 N^2} \frac{\partial \psi'}{\partial z} \right) \tag{A1.7}$$

ie.

$$\underline{D} = \underline{\underline{\epsilon}} \nabla \psi' \tag{A1.8}$$

where $\underline{\underline{\epsilon}}$ is now defined by

$$\begin{aligned} \epsilon_{11} = \epsilon_{22} &= \frac{\rho_s}{\rho_0} \\ \epsilon_{33} &= \frac{\rho_s}{\rho_0} \frac{f_0^2}{N^2} \end{aligned} \tag{A1.9}$$

Note that for uniform N^2 and an incompressible atmosphere the dielectric tensors for the omega and potential vorticity equations are equal and furthermore imply a purely vertical "polarisation".

APPENDIX 2

The compressible uniform ball solution

Bishop and Thorpe (1994) present solutions for the stream function attributable to a uniform ball of quasi-geostrophic potential vorticity, which leads to the incompressible Poisson problem. We here derive a compressible solution analogous to theirs, following their notation. The solution for the inside of the ball, $r<b$, may be found as a particular integral of the radial equation in the transformed variable φ

$$\varphi'' + \frac{2}{r}\varphi' - \frac{1}{D_\rho^2}\varphi = q(r) \qquad \textbf{(A2.1)}$$

where $q(r)$ is a radial distribution of forcing, in this case constant. The homogeneous Helmholtz equation has solutions of the form $\exp(\pm r/D_\rho)/r$ so that Eq. (A2.1) can be solved by the Wronskian method given by Morse and Feshbach (1953), p.529-530, or by matching to the outer region solution to yield

$$\varphi = q\frac{D_\rho^3}{r}\left((1+\frac{b}{D_\rho})\exp(-\frac{b}{D_\rho})\sinh(\frac{r}{D_\rho}) - \frac{r}{D_\rho}\right) \qquad \textbf{(A2.2)}$$

The outer region solution for $r>b$ is of the form given by Eq (10); matching φ and φ' at b gives

$$\varphi = q\frac{D_\rho^3}{r}\left(b\cosh(\frac{b}{D_\rho}) - D_\rho\sinh(\frac{b}{D_\rho})\right)\exp\left(-\frac{r}{D_\rho}\right) \qquad \textbf{(A2.3)}$$

This solution differs from the solution to the Poisson ball problem in that the solution in the outer region is not identical to the point source solution, though in the limit as $D_\rho \to \infty$ the two problems become degenerate. However, in practice it is readily found by Taylor expansion that the outer solution is well approximated (to within 1.5% even for b=1000km) by the simpler expression

$$\varphi = -\frac{qb^3}{3r}\exp\left(-\frac{r}{D_\rho}\right) \qquad \textbf{(A2.4)}$$

The expressions for ϕ, corresponding to their ψ, follow from Eq. (7).

It should be noted that this problem is not physically identical to the incompressible Poisson problem because it is defined in terms of the transformed variable, and thus differs slightly in that the physical source is $q\exp(-z/2H_\rho)$. There is a very small increase in this volume-integrated source compared to the incompressible case, but the major part of the difference is a vertically aligned dipole, and so the outer region solution differs with a leading term $1/r^2$, which may for most purposes be ignored. Similarly, the

internal solution could also be approximated by spherical harmonic expansion, though this level of detail is not pursued here as it is of little physical importance.

REFERENCES

Bishop, C. and Thorpe, A. J. 1994 Potential vorticity and the electrostatics analogy: quasi-geostrophic theory. *Q. J. R. Meteorol. Soc.*, **120**, 713-731.

Charney, J. G. 1963 Numerical experiments in atmospheric hydrodynamics. *Proc. Symp. Appl. Math.*,**15**, 289-310.

Clough, S. A. and Davitt, C. S. A. 1994 Development of an Atlantic frontal wave during IOP 3 of Fronts 92, in '*The Life Cycles of Extratropical Cyclones*', Proceedings of an International Symposium, Geophysical Institute, University of Bergen, 27th June - 1st July 1994, (eds. S. Grønås and M. A. Shapiro) vol. II, 151-156.

Eliassen, A. 1959 On the formation of fronts in the atmosphere. pp. 277-287 in *The Atmosphere and the Sea in Motion*, N. Y. Rockefeller Institute Press.

Eliassen, A. 1962 On the vertical circulation in frontal zones. *Geofys. Publikasjoner*, **24** (No. 4), 147-160.

Eliassen, A. 1984 Geostrophy. *Q. J. R. Meteorol. Soc.*, **110**, 1-12.

Hogg, N. G. and Stommel, H. M. 1985 The heton, and elementary interaction between discrete baroclinic geostrophic vortices, and its implications concerning eddy heat-flow. *Proc. R. Soc. Lond.* **A397**, 1-20.

Hogg, N. G. and Stommel, H. M. 1985 Hetonic explosions: the breakup and spread of warm pools as explained by baroclinic point vortices. *J. Atmos. Sci.*, **42**, 1465-1476.

Hoskins, B. J. and Bretherton, F. P. 1972 Atmospheric frontogenesis models: mathematical formulation and solution. *J. Atmos. Sci.*, **29**, 11-37.

Hoskins, B. J., Draghici, I. Davies, H. C. 1978 A new look at the ω-equation. *Q. J. R. Meteorol.* and *Soc.*, **104**, 31-38.

Hoskins, B. J., McIntyre, M. I. and Robertson, W. A. 1985 On the use and significance of isentropic potential vorticity maps. *Q. J. R. Meteorol. Soc.*, **111**, 877-946.

Keyser, K., Reeder, M. J. and Reed, R. J. 1988 A generalization of Pettersen's frontogenesis function and its relation to the forcing of vertical motion, *Mon. Wea. Rev.*, **116**, 762-780.

Lorrain, P., D. P. Corson and F. Lorrain 1988 *Electromagnetic fields and waves.* W. H. Freeman and Company, New York.

Morse, P.M. and Feshbach, H. 1953 *Methods of Theoretical Physics.* McGraw Hill Book Company, Inc.

Stakgold, I. 1968 *Boundary Value Problems of Mathematical Physics*, vol.II. MacMillan, New York.

Thorpe, A. J. and Bishop, C. H. 1995 Potential vorticity and the electrostatic analogy: Ertel-Rossby formulation. *Q. J. R. Meteorol. Soc.*, in press.

Williams, G. P. 1988 The dynamical range of global circulations. *Climate Dynamics, 2*, 205-260.

CURRENT JCMM INTERNAL REPORTS

This series of JCMM Internal Reports, initiated in 1993, contains unpublished reports and also versions of articles submitted for publication. The complete set of Internal Reports is available from the National Meteorology Library on loan, if required.

1. **Research Strategy and Programme.**
   K A Browning et al
   January 1993

2. **The GEWEX Cloud System Study (GCSS).**
   GEWEX Cloud System Science Team
   January 1993

3. **Evolution of a mesoscale upper tropospheric vorticity maximum and comma cloud from a cloud-free two-dimensional potential vorticity anomaly.**
   K A Browning
   January 1993

4. **The Global Energy and Water Cycle**
   K A Browning
   July 1993

5. **Structure of a midlatitude cyclone before occlusion.**
   K A Browning and N Roberts
   July 1993

6. **Developments in Systems and Tools for Weather Forecasting.**
   K A Browning and G Szejwach
   July 1993

7. **Diagnostic study of a narrow cold frontal rainband and severe winds associated with a stratospheric intrusion.**
   K A Browning and R Reynolds
   August 1993

8. **Survey of perceived priority issues in the parametrizations of cloud-related processes in GCMs.**
   K A Browning
   September 1993

9. **The Effect of Rain on Longwave Radiation.**
   I Dharssi
   September 1993

10. **Cloud Microphysical Processes - A Description of the Parametrization used in the Large Eddy Model.**
H Swann
July 1994

11. **An Appreciation of the Meteorological Research of Ernst Kleinschmidt.**
A J Thorpe
May 1992

12. **Potential Vorticity of Flow Along the Alps.**
A J Thorpe, H Volkert and Dietrich Heimann
August 1992

13. **The Representation of Fronts.**
A J Thorpe
January 1993

14. **A Parametrization Scheme for Symmetric Instability: Tests for an Idealised Flow.**
C S Chan and A J Thorpe
February 1993

15. **The Fronts 92 Experiment: a Quicklook Atlas.**
Edited by T D Hewson
November 1993

16. **Frontal wave stability during moist deformation frontogenesis. Part 1. Linear wave dynamics**
C H Bishop and A J Thorpe
May 1993

17. **Frontal wave stability during moist deformation frontogenesis. Part 2. The suppression of non-linear wave development.**
C H Bishop and A J Thorpe
May 1993

18. **Gravity waves in sheared ducts.**
S Monserrat and A J Thorpe
October 1993

19. **Potential Vorticity and the Electrostatics Analogy: Quasi-Geostrophic Theory.**
C Bishop and A J Thorpe
November 1993

20. **Recent Advances in the Measurement of Precipitation by Radar.**
A J Illingworth
April 1993

21. **Micro-Physique et Givrage. Cloud Microphysics and Aircraft Icing.**
A J Illingworth
May 1993

22. **Differential Phase Measurements of Precipitation.**
M Blackman and A J Illingworth
May 1993

23. **Estimation of Effective Radius of Cloud Particles from the Radar Reflectivity.**
N I Fox and A J Illingworth
May 1993

24. **A Simple Method of Dopplerising a Pulsed Magnetron Radar.**
L Hua, A J Illingworth and J Eastment
November 1993

25. **Radiation and Polar Lows.**
George C Craig
February 1994

26. **Collected preprints submitted to International Symposium on the Life Cycles of Extratropical Cyclones; Bergen, Norway, 27 June - 1 July 1994**
April 1994

27. **Convective Frontogenesis**
Douglas J Parker and Alan J Thorpe
April 1994

28. **Improved Measurement Of The Ice Water Content In Cirrus Using A Total Water Evaporator**
Philip R A Brown and Peter N Francis
April 1994

29. **Mesoscale Effects of a Dry Intrusion within a Vigorous Cyclone**
K A Browning and B W Golding
April 1994

30. **GEWEX Cloud System Study, Science Plan**
May 1994

31. **Parametrization of Momentum Transport by Convectively Generated Gravity Waves**
R Kershaw
February 1995

32. **Mesoscale Modelling Newsletter, No. 5**
May 1994

33. **Observations of the mesoscale sub-structure in the cold air of a developing frontal cyclone**
K A Browning, S A Clough, C S A Davitt, N M Roberts and T D Hewson
May 1994

34. **Longwave Radiative Forcing of a Simulated Tropical Squall Line**
Imtiaz Dharssi
July 1994

35. **On the nature of the convective circulations at a kata-cold front**
K A Browning
September 1994

36. **Collected preprints of papers submitted to the COST-75 International Seminar on Advanced Weather Radar Systems, Brussels, 20-23 September 1994**
November 1994

37. **Use of satellite imagery to diagnose events leading to frontal thunderstorms: Parts I and II of a case study**
K A Browning and N M Roberts
November 1994

38. **The role of spaceborne millimetre-wave radar in the global monitoring of ice cloud**
P R A Brown, A J Illingworth, A J Heymsfield, G M McFarquhar, K A Browning and M Gosset
December 1994

39. **Potential Vorticity Inversion**
Michal Ziemianski
October 1994

40. **Theory of mature tropical cyclones; A comparison between Kleinschmidt (1951) and Emanual (1986)**
Suzanne L Gray
December 1994

41. **Dispersion and removal of pollutants during the passage of an atmospheric frontal system**
N R Gimson
December 1994

42. **The role of snow sublimation in frontogenesis**
D J Parker and A J Thorpe
December 1994

43. **Potential vorticity and the electrostatics Analogy: Ertel-Rossby formulation**
A J Thorpe and C H Bishop
December 1994

44. **Mesoscale aspects of extratropical cyclones: an observational perspective**
K A Browning
January 1995

45. **A Polar Low Outbreak: Evolution and Mesoscale Structures**
T D Hewson, G C Craig and C Claud
February 1995

46. **Generation of near-surface gusts by deep convection**
K Nakamura and R Kershaw
April 1995

47. **Attribution concepts applied to the omega equation**
S A Clough, C S A Davitt and A J Thorpe
June 1995

Met Office Joint Centre for Mesoscale Meteorology Department of Meteorology
University of Reading PO Box 243 Reading RG6 6BB United Kingdom
Tel: +44 (0)118 931 8425 Fax: +44 (0)118 931 8791
www.metoffice.com